Synthesis and Quantitative Structure−Activity Relationship of Hydrazones of *N*-Amino-*N*′-hydroxyguanidine as Electron Acceptors for Xanthine Oxidase

Peteris Prusis,[†] Maija Dambrova,[†] Victor Andrianov,[‡] Eugene Rozhkov,[‡] Valentina Semenikhina,[‡] Irena Piskunova,[‡] Enock Ongwae,[†] Torbjörn Lundstedt,[§] Ivars Kalvinsh,[‡] and Jarl E. S. Wikberg*[,†]

Department of Pharmaceutical Biosciences, Division of Pharmacology, Uppsala University, Uppsala SE751 24, Sweden, Department of Medicinal Chemistry, Latvian Institute of Organic Synthesis, Riga, Latvia, and Melacure Therapeutics AB and Department of Pharmaceutical Chemistry, Uppsala University, Uppsala SE751 24, Sweden

Received December 4, 2003

A series of new *N*-hydroxyguanidines were synthesized and tested for electron acceptor activity on bovine milk xanthine oxidase using xanthine as reducing substrate. Manual inspection of the structure−activity data revealed that molecules containing nitro groups ("set A") show a different structure−activity relationship pattern compared to non-nitro compounds ("set B"). Accordingly separate QSAR models were built and validated for the two sets. Substantial differences were found in properties governing acceptor activity for the models, the only common property being sterical access to the imino nitrogen atom of the hydroxyguanidinimines. For set A molecules the presence of a nitro substituent at a certain distance range from the hydroxuguanidino group was most important. In addition, the presence of a nitro group in the ortho position interacting with NH_2 of the hydroxyguanidino group, and the mutual geometry of the phenyl ring, hydroxyguanidine, and imine groups was important for this set. By contrast, for set B molecules the acceptor activity was most influenced by the geometry of methoxy groups and the size and geometry of meta and para substituents of the phenyl ring.

Introduction

Xanthine oxidase (EC 1.1.3.22) (XO) is a complex molybdoflavoprotein that catalyzes the hydroxylation of xanthine and hypoxanthine by utilizing molecular oxygen as an electron acceptor.[1,2] During a period of restricted supply of oxygen (i.e., ischemia), xanthine and hypoxanthine will accumulate in tissue. A subsequent restoration of the delivery of oxygen may then lead to an increase in the oxidation of xanthine and hypoxanthine by XO, under a massive formation of superoxide and other oxygen-derived free radicals.[3,4] Such XO-generated reactive oxygen species are suggested to have pathogenic roles in a variety of clinical disorders, including the so-called ischemia/reperfusion syndrome.[5,6]

Several approaches have been tried to prevent XO-mediated tissue damage.[7−9] Thus, the XO inhibitor allopurinol was shown to improve cardiac function in patients undergoing coronary artery bypass surgery.[10,11] Pentoxifylline, a novel inhibitor of XO, was also shown to reduce lipid peroxidation and to ameliorate histopathological signs of injury in experimental rat intestinal ischemia-reperfusion.[12] Another is to compete for reducing equivalents, thereby diminishing the likelihood for the reduction of molecular oxygen by XO. Methylene blue was shown to function as an alternative electron acceptor at XO and to be capable of inhibiting the reduction of molecular oxygen to its superoxide radical.[13,14] Supposedly by virtue of this mechanism methylene blue prevented the pulmonary injury otherwise elicited in experimental intestinal ischemia−reperfusion.[14,15]

It is known that the specificities of XO active compounds are relatively low for substrates that undergo reduction and oxidation. In addition to the natural substrates, XO is able to oxidize and reduce a large number of compounds that show quite varying structures. In particular, nitrogen-containing substrates show large structural variations.[16,17] Inhibitors of XO include allopurinol and alloxanthine, which are analogues of the XO's natural purine substrates. Allopurinol (one of the most studied XO active compounds) becomes oxidized by XO, and then it inhibits the enzyme by forming a tight complex with the molybdenum of the enzyme's active site.[7,18] Electron acceptors of XO have been investigated to a far lesser extent. It has been observed for most of the evaluated cases that the reduction of the electron-accepting substance is greatly inhibited by the presence of oxygen. Accordingly the reduction of such compounds can be observed essentially only under anaerobic conditions.[19−21] However, methylene blue was found to be reduced aerobically, with the reaction proceeding at the iron−sulfur center of XO.[22] Detailed structure−activity relationships for XO-mediated reductions have earlier been studied only for aromatic nitro compounds and benzoquinones.[19,20,23]

We have shown previously that some aromatic hydrazones of *N*-hydroxyguanidine may become reduced to the corresponding guanidines by XO at the enzyme's molybdenum center.[24,25,26] We found that a novel *N*-hydroxyguanidine derivative *N*-(2-chloro-3,4-dimethoxybenzylideneamino)-*N*′-hydroxyguanidine (PR5) was particularly effective functioning as an alternative electron acceptor in the XO-catalyzed oxidation of xanthine, the PR5 being effective even under aerobic conditions.[26]

* To whom correspondence should be addressed. Telephone: +46-18-4714238. Fax: +46-18-559718. E-mail: Jarl.Wikberg@farmbio.uu.se.
[†] Division of Pharmacology, Uppsala University.
[‡] Latvian Institute of Organic Synthesis.
[§] Melacure Therapeutics AB and Department of Pharmaceutical Chemistry, Uppsala University.

10.1021/jm031127c CCC: $27.50
Published on Web 05/08/2004

Pharmacological testing of PR5 revealed furthermore that it had a remarkable protective effect against the induction of myocardial necrosis and life-threatening arrhythmias in a heart ischemia and reperfusion model, where the rat's left coronary artery was first occluded during a timed interval and then reopened.[27]

In the present study we synthesized a series of new *N*-amino-*N*′-hydroxyguanidines and tested them for electron acceptor activity in the XO-catalyzed oxidation of xanthine. We also performed quantitative structure−activity relationship studies using a novel 3D-QSAR approach. The novel XO electron-accepting *N*-hydroxyguanidines might find use for the prevention of free radical formation to protect tissues during conditions related to ischemia−reperfusion.

Results and Discussion

Synthesized Compounds and Their Activities. The 51 compounds synthesized herein are listed in Table 1, together with their XO electron acceptor activity. The above-mentioned substance PR5 (**40**) is also included (Table 1).

From Table 1 it can be seen that the two compounds (**6**, **14**) having the highest acceptor activity contain two nitro groups each. In fact, out of the four compounds that contain two nitro groups, three (**6**, **14**, **16**) show very high acceptor activities while one (**11**) shows relatively low activity. However, there are also active compounds (**38**, **40**, **45**) that do not contain nitro groups. A common feature of the latter ones is the presence of several methoxy groups. Still, there are several compounds that contain several methoxy groups that show very low acceptor activity. Moreover, nitro-group-containing compounds having several methoxy groups generally show quite low acceptor activity.

QSAR Modeling. The above SAR analysis showed that it was not possible to derive a simple relationship between the presence and absence of different substituents on the *N*-hydroxyguanidines and their activities on the XO enzyme. We assumed that this was due to spatial differences in the molecules rather than the presence or absence of some substituents at particular positions. To understand the three-dimensional properties that determine the activities of hydroxyguanidines, we performed 3D-QSAR analysis. The three-dimensional structures of compounds were calculated by semiempirical modeling, using the X-ray structure of *N*-benzilideneamino-*N*′-hydroxyguanidine[28] as the starting template. In addition to the semiempirical calculations, we also performed a simple conformational search for each molecule. The molecules having the calculated lowest heat of formation was chosen for the evaluation.

To avoid problems of three-dimensional alignment of the molecules in space, we used a novel alignment-independent 3D-QSAR technology.[29] Initial elaboration of the data showed that it was not possible to obtain good correlation if all the substances were included in one data set. Careful inspection of the structures and comparison with the binding data suggested that compounds containing nitro groups might behave differently from the remaining compounds. Thus, we generated separate QSAR models for compounds containing NO_2 group(s) (**1**−**17**, set A) and the remaining compounds (**18**−**51**, set B). This led to good QSAR models for both sets.

Table 1. Structures of Hydroxyguanidines and Their Xanthine Oxidase Electron Acceptor Activity[a]

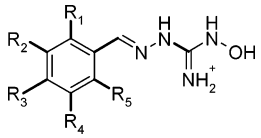

compd	R_1	R_2	R_3	R_4	R_5	acceptor activity ± SEM
1	H	NO_2	H	H	H	24.4 ± 5.3
2	H	NO_2	Cl	H	H	42.1 ± 3.3
3	H	H	NO_2	H	H	94.2 ± 5.8
4	OH	H	H	NO_2	H	25.8 ± 3.3
5	NO_2	H	H	H	H	56.4 ± 6.5
6	NO_2	H	NO_2	H	H	295.7 ± 16.0
7	Cl	H	H	H	NO_2	44.0 ± 4.7
8	NO_2	H	H	OH	H	31.5 ± 5.9
9	OCH_3	H	H	OCH_3	NO_2	47.3 ± 7.3
10	OCH_3	OCH_3	H	NO_2	H	0.8 ± 1.2
11	OCH_3	OCH_3	H	NO_2	NO_2	52.9 ± 9.4
12	OCH_3	OCH_3	H	H	NO_2	22.0 ± 5.3
13	H	NO_2	Br	H	H	35.0 ± 2.8
14	NO_2	NO_2	H	H	Cl	216.3 ± 3.0
15	NO_2	Cl	H	H	Cl	68.3 ± 10.0
16	NO_2	H	H	H	NO_2	154.5 ± 3.0
17	Cl	OCH_3	OCH_3	H	NO_2	48.8 ± 2.4
18	Br	H	H	H	H	72.9 ± 9.6
19	OCH_3	H	H	OCH_3	H	42.3 ± 7.2
20	H	H	$N(CH_3)_2$	H	H	41.0 ± 8.4
21	H	Cl	H	H	H	45.4 ± 7.2
22	H	H	Cl	H	H	57.9 ± 4.2
23	H	H	Br	H	H	82.1 ± 5.6
24	H	H	$N(C_2H_5)_2$	H	H	62.1 ± 3.3
25	OCH_3	H	H	H	OCH_3	13.2 ± 8.5
26	F	H	H	H	H	49.6 ± 9.0
27	OCH_3	H	H	H	H	59.7 ± 6.7
28	H	OCH_3	H	H	H	55.0 ± 8.2
29	Cl	H	H	H	H	90.2 ± 8.1
30	H	H	F	H	H	43.2 ± 2.3
31	H	F	H	H	H	56.2 ± 8.3
32	H	Br	OCH_3	H	H	35.6 ± 3.5
33	OCH_3	H	OCH_3	OCH_3	H	29.7 ± 2.9
34	H	OCH_3	OCH_3	OCH_3	H	54.6 ± 8.8
35	H	H	OCH_3	H	H	50.9 ± 5.7
36	OCH_3	OCH_3	OCH_3	H	H	81.5 ± 3.9
37	OCH_3	H	OCH_3	H	OCH_3	10.8 ± 1.2
38	Br	OCH_3	OCH_3	OCH_3	H	119.5 ± 12.9
39	H	OCH_3	H	OCH_3	H	30.7 ± 5.1
40	Cl	OCH_3	OCH_3	H	H	155.6 ± 16.4
41	OCH_3	H	OCH_3	Br	H	16.3 ± 3.8
42	OCH_2O		H	H	H	44.7 ± 4.1
43	OH	H	OH	H	H	72.9 ± 2.9
44	OH	OH	H	H	H	43.7 ± 5.0
45	OH	H	OCH_3	H	OCH_3	101.7 ± 2.7
46	OH	OCH_3	H	H	H	45.5 ± 3.9
47	OH	H	H	H	H	33.8 ± 1.0
48	H	H	OH	H	H	64.2 ± 2.9
49	OH	OH	OH	H	H	40.5 ± 6.9
50	H	OH	OCH_3	H	H	68.9 ± 7.6
51	OH	OCH_3	H	Br	H	72.4 ± 5.0

[a] All compounds are tosylates. The bonds shown with bold lines in the structure indicate that they were rotated during the conformational searches.

The results from the modeling of both data sets, obtained by applying the PLS algorithm, are shown in Table 2. In the modeling process, different probe atoms were elaborated for the creation of the MIFs. For set A, the best results were obtained using just chlorine (CL) probe atoms, while for set B, the (hydrophobic) DRY, carbonyl (O), and amide (N1) probe atoms[29] proved to be satisfactory. Moreover, the use of three probe atoms in the latter case required application of

Table 2. PLS Modeling Results[a]

parameter	data set	
	set A	set B
probe atoms	CL	DRY, N1, O
number of nodes	150	50
number of LVs	2	3
R^2	0.84	0.87
SDEC	30.4	12.5
Q^2	0.59	0.65
SDEP	48.2	17.5
external SDEP	31.6	14.4

[a] For details, see text.

variable selection. The GOLPE variable selection used herein was validated by applying it to a subset of data and predicting the activities of the excluded data (see Table 2.)

Interpretation of the Models. To understand the meaning of the models, we explored the PLS coefficient plots of each GRIND descriptor block separately. The descriptors that had high positive or negative values were considered to be important. The important descriptors were arranged into groups by collecting descriptors originating from similar distances between MIF nodes and having the same direction of PLS coefficients. The meaning of these groups of coefficients, and also of individual descriptors, was investigated by assessing their origins (in three-dimensions) in the MIFs for every particular molecule. During this investigation, we considered splitting or joining groups of coefficients into subgroups if the physical meaning of the coefficient appeared to be similar or different. An example of the analysis is shown in Figure 1.

Thus, as shown in Figure 1A the descriptors of the DRY−DRY autocorrelogram could be divided into six groups according to the PLS coefficient plot. The three-dimensional analysis of these groups are exemplified in Figure 1B−E. Panels B and C illustrate compounds **38** and **40** showing high acceptor activity, while panels D and E illustrate compounds **39** and **41** showing low acceptor activity. In all four cases, the lines representing GRIND descriptors connect MIFs around the phenyl ring. Shorter GRINDs of groups 1 and 2 connect MIFs on one side of the phenyl ring, while little longer GRINDs of groups 3 and 4 connect MIFs from opposite sides of the phenyl ring. For the substances shown in Figure 1B,C the red color of the GRIND descriptors indicates that descriptors have high values, while for the substances shown in Figure 1D,E the GRIND descriptors have a blue color indicating low values of these descriptors. Thus, these GRIND descriptors have high values if MIFs around the phenyl ring have high values and vice versa. From Figure 1 it can be seen that high values of MIFs around the phenyl ring are associated with methoxy substituents, where the plane of the C−O−C atoms of this group is not parallel to the plane of the phenyl ring. Thus, the positive correlation of these descriptors with activity indicates that methoxy substituents, which are not coplanar with the phenyl ring, increase acceptor activity.

Performing this analysis for both data sets showed that although some similarities exist, there are important differences, which require a separate discussion for each of the data sets. Below, we first discuss the set B model followed by a discussion for the set A model.

Compounds without Nitro Groups (Set B Model). As already discussed above and illustrated graphically in Figure 1 for four of the molecules in set B, the most important property for high acceptor activity is that methoxy substituents should not be coplanar with the phenyl ring. This property emerged also from analysis of DRY−O and DRY−N1 cross-correlograms.

The second main property increasing acceptor activity was that access to the nitrogen atom of the imine should be sterically hindered.

A third important property also appears to be the size and geometry (with respect to the iminohydroxyguanidine group) of the para and meta substituents of the phenyl. If these substituents are within a certain size range (e.g., Cl−, Br−, and in some cases CH_3O−), they in most cases improve acceptor activity. On the other hand, substituents outside this size range (F−, $(CH_3)_2N$−, and $(C_2H_5)_2N$−) have no or a diminishing effect on the activity.

Besides these three main properties influencing acceptor activity, a few other features of the molecules were found to be important, giving a smaller effect on the activity. For example, the composition, orientation, and geometry of meta and ortho substituents, as well as the geometry of the hydroxyguanidinium imine group, appear to be of importance.

Nitro-Group-Containing Compounds (Set A Model). Several properties were found to play major roles for the XO electron acceptor activity of arylhydrazones of *N*-hydroxyguanidines having nitro group substituents in their aromatic moiety. The most important property causing an increase of activity is the presence of nitro groups at a certain distance (typically at R_1, R_3, or R_4 position; see Table 1) from the hydroxyguanidino moiety. Very important for activity was the presence of a nitro group at position R5, which interacts with the NH_2 group of the hydroxyguanidine. Also important was the mutual geometry of the hydroxyguanidine and the phenyl ring. It was found that if the planes of the guanidine and phenyl ring were coplanar, it led to a decrease in the electron acceptor activity. At the same time the hydroxyguanidine and imine planes should be in the same plane in order to yield high activity. Steric access to the nitrogen atom of the imino group was also found to be important for acceptor activity, as found for the set B compounds lacking nitro groups, although to a lesser extent.

Conclusion

The results show that it is not possible to obtain predictive models when all hydroxyguanidines of the present series are modeled together. However, good predictive models can be obtained when the compounds containing nitro groups (set A) and the compounds lacking a nitro group (set B) were modeled separately. When we compared the results obtained from the interpretation of both sets A and B models, we found that steric access of the imino group to the nitrogen atom was important for both cases. No other evident similarities were found for the two models. One possible explanation for this might be that nitro- and non-nitro compounds have different but partially overlapping binding pockets centered around the imino group.

The present QSAR models may be amenable for the design of improved xanthine oxidase electron acceptors.

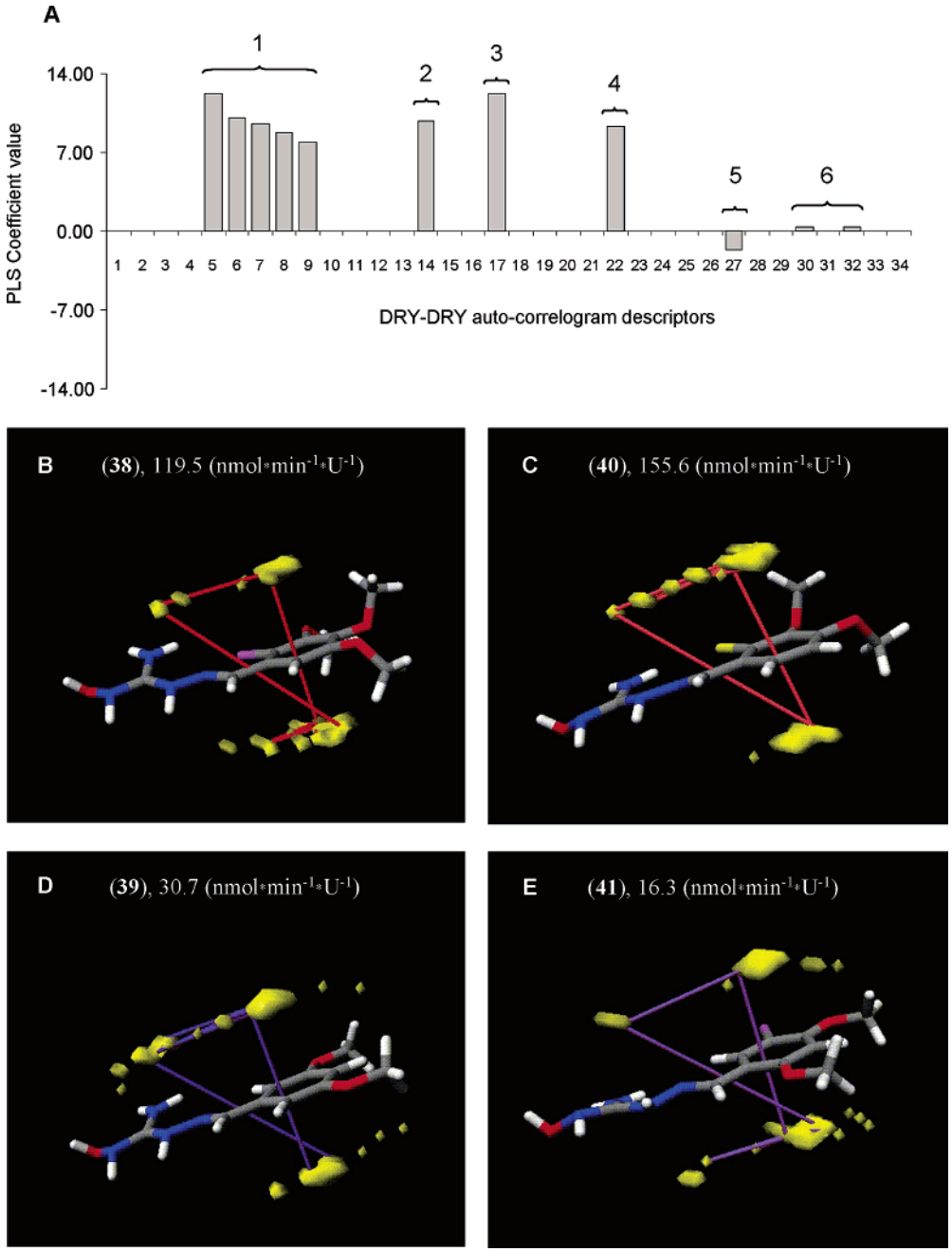

Figure 1. Example of the interpretation of the PLS model for acceptor activity of set B: (A) PLS coefficients of GRIND descriptors for the DRY−DRY autocorrelogram; (B−E) three-dimensional visualization of GRIND descriptors. Compound numbers (according to Table 1) are shown in parentheses, followed by the experimentally determined acceptor activity. MIFs are shown in yellow. The lines connecting two nodes of MIFs indicate the origin of GRIND descriptors, which were calculated as the product of the two MIF nodes. The colors of these lines are coded so that they gradually change from blue for a low value of the variable to red for a high value. Note that for the active compounds, bromine and chlorine atoms are located close to the nitrogen atom of the CH═N group (panels B and C, respectively), while for the inactive compounds this location is taken by a much smaller hydrogen (panels D and E). The larger chlorine and bromine atoms hinder the probe atom from accessing the nitrogen of the CH═N group in the active compounds, whereas the smaller hydrogen found in the inactive compounds does not hinder the probe atoms from interacting with the nitrogen of the CH═N group.

Such compounds might be useful to reduce the formation of toxic superoxide. PR5 (**40**) was reported to be a strong cardioprotector in a heart infarction model in the rat.[27] It was speculated that the effect was due to the xanthine oxidase electron-accepting property of the compound, which would reduce the formation of toxic superoxide during the so-called ischemia−reperfusion syndrome associated with heart infarction.[26] However, the mechanism of action of PR5 (**40**) is still elusive, while its dehydroxy metabolite, termed ME10092, was equally effective as PR5 (**40**) in the very same heart infarction model.[30] Guanoxabenz is a structurally related hydroxyguanidine that has been used clinically as an antihypertensive.[31] The design of improved xanthine oxidase electron acceptors may lead to compounds with new interesting pharmacological profiles.

Experimental Section

Organic Synthesis. Compounds **1**,[33] **2**,[33] **28**,[32] **19**,[33] **35**,[34] **36**,[34] **37**,[34] **33**,[34] **34**,[34] **50**,[35] **31**,[35] **47**,[36] **49**,[36] and **45**[37] (see Table

1) were synthesized according to the methods described in the literature. Melting points were determined with the Fisher table. ^{1}H NMR spectra were obtained on a Bruker WH 90/DS in DMSO-d_6. Thin-layer chromatography was performed on Merck precoated silica gel 60 F_{254} sheets.

General Procedure for the Synthesis of Hydrazones of *N*-Amino-*N*′-hydroxyguanidine. An equimolar amount (10 nmol) of *N*-amino-*N*′-hydroxyguanidine *p*-toluenesulfonate and the appropriate carbonyl compound were heated under reflux in ethanol (15 mL) for 0.1−1 h. Reactions were monitored by TLC. When a reaction was complete, the product was precipitated after cooling (2 h at 0 °C) or in some cases isolated by concentrating the reaction mixture in a vacuum, and the product crystallized using a suitable solvent. The detailed description for the synthesis procedure is given for compound **40**. The results of the synthesis and the analytical data for all compounds are summarized in Supporting Information.

***N*-(2-Chloro-3,4-dimethoxybenzylideneamino)-*N*′-hydroxyguanidine tosylate (40).** A solution of 2-chloro-3,4-dimethoxybenzaldehyde (2.0 g, 10 mmol) and *N*-amino-*N*-hydroxyguanidine *p*-toluenesulfonate (2.6 g, 10 mmol) in ethanol (15 mL) was heated at 50−60 °C for 5−8 min. After 2 h at 0 °C, the precipitate was filtered off and gave 2.9 g (62%) of product. The filtrate was evaporated, and an additional portion of product was obtained. Yield 93%; mp 95−97 °C; ^{1}H NMR δ 2.29 (3H, s), 3.76 (3H, s), 3.91 (3H, s), 7.13 (2H, d), 7.16 (1H, d), 7.49 (2H, d), 8.09 (1H, d), 8.22 (2H, s), 8.58 (1H, s), 10.11 (1H, br. s), 11.34 (1H, br s), 11.76 (1H, br. s). Anal. ($C_{10}H_{13}ClN_4O_3 \cdot C_7H_8O_3S \cdot H_2O$) C, H, N.

Electron Acceptor Activity Assay. Reduction rates of *N*-hydroxyguanidines were determined under anaerobic conditions. An amount of 1 mL of a mixture containing 50 μM *N*-hydroxyguanidine compound, 50 μM xanthine, 0.05 units/mL bovine milk xanthine oxidase (obtained from Sigma, St. Louis, MO) in 25 mM Tris-HCl, 1 mM EDTA, pH 7.5, was incubated at 25 °C in a Helma sealable cuvette for anaerobic applications. Incubation mixtures where *N*-hydroxyguanidine was excluded served as controls. Prior to incubation, all solutions were gassed for at least 10 min with argon. The reaction was started by the injection of milk xanthine oxidase into the cuvette. The anaerobic control readings were subtracted from each test reading. Values in Table 1 represent the mean of three separate determinations expressed as μmol of uric acid formed (calculated from the increase in absorption at 295 nm, $\epsilon_{\text{uric acid}} = 12.4 \pm 0.16$ mmol^{-1} cm^{-1}) per min per unit of xanthine oxidase.

Molecular Modeling. Molecular modeling was done using the SYBYL program.[38] The X-ray structure of 1-(benzylideneamino)-3-hydroxyguanidinium tosylate,[28] obtained from the Cambridge Structural Database,[39] served as an initial template for all molecules. Prior to the calculations, the hydrogens of the X-ray template were substituted with the appropriate chemical groups. Conformational searches were performed by rotating selected bonds by 180°. (The bonds selected for conformational search are shown by bold lines in the structure template in Table 1.) The geometry of each such conformer was then optimized using semiempirical calculations using the PM3 parameter set.[40,41] The calculations were performed using MOPAC[40−42] (keywords applied were PREC DENSITY LOCAL VECT MULLIK PI BONDS GRAPH PM3 T=3600 CHARGE=1) implemented in SYBYL.[38] The conformer for each compound that had the lowest heat of formation was chosen for the QSAR studies.

GRID and GRIND Descriptors. The modeled three-dimensional structure of each molecule was coded into grid independent descriptors (GRIND)[29] using the ALMOND software.[43] GRIND descriptors are independent from spatial alignment of compounds. The calculation of these descriptors involves several steps. Molecular interaction fields (MIFs) on grid points surrounding the molecule are first calculated using the GRID program.[44] This is achieved by placing some probe atom at all nodes of the grid surrounding the molecule. (The distance between grid nodes used this study was 0.5 Å.) Several different probe atoms can be used, thus creating different MIFs. The compounds were kept charged throughout the modeling. A number of grid nodes are then extracted, which show the energetically most favorable interactions and which are as far as possible from each other (see Pastor et al.[29] for details). The number of extracted nodes for each model is shown in Table 2. The products and distances between each two extracted nodes of the same type of MIFs (autocorrelograms) and different types of MIFs (cross-correlograms) are then calculated. From all these products the GRIND descriptors are thereafter chosen, which have a maximum value at specified distance ranges. For set A the probe atom was CL, resulting in a CL−CL autocorrelogram. For set B and all its three subsets, the probe atoms were DRY, N1, and O, resulting in DRY−DRY, N1−N1, and O−O autocorrelograms and DRY−N1, DRY−O, and N1−O cross-correlograms.

PLS and GOLPE. The GRIND descriptors were correlated with the measured biological activities. The presence of a large number of covarying descriptors prompts the use of PLS as the correlation method.[45] PLS transforms the descriptor matrix to a new matrix of lower dimensionality. The descriptors of this new matrix, called latent variables (LV), are orthogonal. The LVs are calculated so that explanation of the descriptor matrix and simultaneously maximum correlation to the activity data are achieved. The goodness of PLS models were evaluated using R^2 and SDEC values.[46] The PLS models were validated using 20 rounds of cross-validation with five random groups. The cross-validation was characterized using Q^2 values[47] and SDEP.[46]

The large number of GRIND descriptors in the case of set B causes a risk for chance correlations. One of the methods to decrease the number of descriptors and thereby reduce the risk for chance correlations is variable selection. In the present work we chose to use the GOLPE variable selection procedure[46] as implemented in the ALMOND program.[43] The GOLPE variable selection was further validated by applying it on a subset of molecules (test set) for both data sets and predicting activities (prediction set) of the remaining compounds. The prediction set was chosen so that it contained $^1/_3$ of all molecules and spanned the activity scale. Thus, for set A, the prediction set contained molecules **7**, **8**, **12**, **14**, **15**, and **17**, but for set B, the prediction set contained molecules **21**, **22**, **23**, **25**, **30**, **34**, **35**, **38**, **39**, **43**, **48**, and **49**. The predictability was assessed by external SDEP values.[46]

Acknowledgment. We express our sincere gratitude to Drs. Manuel Pastor and Gabriele Cruciani for their invaluable help in teaching us ALMOND and GOLPE and to Prof. Sergio Clementi for allowing P.P. to spend time in his laboratory (Department of Chemistry at University of Perugia) to acquire training in QSAR methods. We are also grateful to Prof. D. W. Oliwer (Potchefstroom University, South Africa) for the generous gift of some *N*-hydroxyguanidines used in the preliminary investigations of this study. We also thank M. Davidson-Brogren for technical assistance. This study was supported by the Swedish MRC (Grant 04X-05957), the Åke Wiberg foundation, the Swedish Heart and Lung Foundation, and Melacure Therapeutics AB.

Appendix

Abbreviations. 3D-QSAR, three-dimensional quantitative structure−activity relationship; GRIND, grid independent descriptors; LV, latent variables; MIF, molecular interaction field; PLS, partial least squares projection to latent structures; SAR, structure−activity relationship; SDEC, standard deviation of errors of calculation; SDEP, standard deviation of errors of prediction; XO, xanthine oxidase.

Supporting Information Available: Analytical data for the compounds. This material is available free of charge via the Internet at http://pubs.acs.org.

References

(1) Kooij, A. A re-evaluation of the tissue distribution and physiology of xanthine oxidoreductase. *Histochem. J.* **1994**, *26*, 889−915.
(2) Parks, D. A.; Granger, D. N. Xanthine oxidase: biochemistry, distribution and physiology. *Acta Physiol. Scand.* **1986**, *548*, 87−99.
(3) Thompson-Gorman, S. L.; Zweier, J. L. Evaluation of the role of xanthine oxidase in myocardial reperfusion injury. *J. Biol. Chem.* **1990**, *265*, 6656−6663.
(4) McCord, J. M. Oxygen-derived free radicals in postischemic tissue injury. *N. Engl. J. Med.* **1985**, *12*, 159−163.
(5) Ar'Rajab, A.; Dawidson, I.; Fabia, R. Reperfusion injury. *New Horiz.* **1996**, *4*, 224−234.
(6) Saugstad, O. D. Role of xanthine oxidase and its inhibitor in hypoxia: reoxygenation injury. *Pediatrics* **1996**, *98*, 103−107.
(7) Hille, R.; Massey, V. Tight binding inhibitors of xanthine oxidase. *Pharmacol. Ther.* **1981**, *14*, 249−263.
(8) Xia, Y.; Khatchikian, G.; Zweier, J. L. Adenosine deaminase inhibition prevents free radical-mediated injury in the postischemic heart. *J. Biol. Chem.* **1996**, *271*, 10096−10102.
(9) Flaherty, I. T. Reperfusion injury. *Free Radical Biol. Med.* **1988**, *5*, 409−419.
(10) Castelli, P.; Condemi, A. M.; Brambillasca, C.; Fundaro, P.; Botta, M.; Lemma, M.; Vanelli, P.; Santoli, C.; Gatti, S.; Riva, E. Improvement of cardiac function by allopurinol in patients undergoing cardiac surgery. *J. Cardiovasc. Pharmacol.* **1995**, *25*, 119−125.
(11) Clancy, R. R.; McGaurn, S. A.; Goin, J. E.; Hirtz, D. G.; Norwood, W. I.; Gaynor, J. W.; Jacobs, M. L.; Wernovsky, G.; Mahle, W. T.; Murphy, J. D.; Nicolson, S. C.; Steven, J. M.; Spray, T. L. Allopurinol neurocardiac protection trial in infants undergoing heart surgery using deep hypothermic circulatory arrest. *Pediatrics* **2001**, *108*, 61−70.
(12) Hammerman, C.; Goldschmidt, D.; Caplan, M. S.; Kaplan, M.; Schimmel, M. S.; Eidelman, A. I.; Branski, D.; Hochman, A. Amelioration of ischemia−reperfusion injury in rat intestine by pentoxifylline-mediated inhibition of xanthine oxidase. *J. Pediatr. Gastroenterol. Nutr.* **1999**, *29*, 69−74.
(13) Salaris, S. C.; Babbs, C. F.; Voorhees, W. D., III. Methylene blue as an inhibitor of superoxide generation by xanthine oxidase. *Biochem. Pharmacol.* **1991**, *42*, 499.
(14) Galili, Y.; Ben-Abraham, R.; Weinbroum, A.; Marmur, S.; Iaina, A.; Volman, Y.; Peer, G.; Szold, O.; Soffer, D.; Klausner, J.; Rabau, M.; Kluger, Y. Methylene blue prevents pulmonary injury after intestinal ischemia−reperfusion. *J. Trauma* **1998**, *45*, 222−226.
(15) Weinbroum, A. A.; Kluger, Y.; Shapira, I.; Rudick, V. Methylene blue abolishes aortal tone impairment induced by liver ischemia−reperfusion in a dose response manner: an isolated-perfused double-organ rat model study. *Shock* **2001**, *15*, 226−230.
(16) Bray, R. C. Molybdenum hydroxylases. In *The Enzymes*; Boyer, P. D., Ed.; Academic Press: New York, 1976; pp 299−419.
(17) Rajagopalan, K. V. Xanthine oxidase and aldehyde oxidase. In *The Enzymatic Basis of Detoxication*; Jakoby, W. B., Ed.; Academic Press: New York, 1980; pp 295−309.
(18) Robins, R.; Revankar, G. R.; O'Brien, D. E.; Springer, R. H.; Novinson, T.; Albert, A.; Senga, K.; Miller, J. P.; Streeter, D. G. Purine analog inhibitors of xanthine oxidase−structure activity relationships and proposed binding of the molybdenum cofactor. *J. Heterocycl. Chem.* **1985**, *22*, 601−634.
(19) Tatsumi, K.; Shigeyuki, K.; Yoshimura, H.; Kawazoe, Y. Susceptibility of aromatic nitro compounds to xanthine oxidase-catalyzed reduction. *Chem. Pharm. Bull.* **1978**, *26*, 1713−1717.
(20) Clarke, E. D.; Goulding, K. H.; Wardman, P. Nitroimidazoles as anaerobic electron acceptors for xanthine oxidase. *Biochem. Pharmacol.* **1982**, *31*, 3237−3242.
(21) Bauer, S. L.; Howard, P. C. The kinetics of 1-nitropyrene and 3-nitrofluoranthene metabolism using bovine liver xanthine oxidase. *Cancer Lett.* **1990**, *54*, 37−42.
(22) Kelner, M. J.; Bagnell, R.; Hale, B.; Alexander, N. M. Potential of methylene blue to block oxygen radical generation in reperfusion injury. *Basic Life Sci.* **1988**, *49*, 894−893.
(23) Lusthof, K. J.; Richter, W.; de Mol, N. J.; Janssen, L. H. M.; Verboom, W.; Reinhoudt, D. N. Reductive activation of potential antitumor bis-aziridinylbenzoquinones by xanthine oxidase: competition between oxygen reduction and quinone reduction. *Arch. Biochem. Biophys.* **1990**, *277*, 137−142.
(24) Dambrova, M.; Uhlén, S.; Welch, C. J.; Prusis, P.; Wikberg, J. E. S. Characterization of the enzymatic activity for biphasic competition by guanoxabenz 1-(2,6-dichlorobenzylidene-amino)-3-hydroxyguanidine) at alpha2-adrenoceptors. II. Description of a xanthine-dependent enzymatic activity in spleen cytosol. *Biochem. Pharmacol.* **1998**, *56*, 1121−1128.
(25) Dambrova, M.; Uhlén, S.; Welch, C. J.; Wikberg, J. E. S. Identification of an *N*-hydroxyguanidine reducing activity of xanthine oxidase. *Eur. J. Biochem.* **1998**, *257*, 178−184.
(26) Dambrova, M.; Baumane, L.; Kiuru, A.; Kalvinsh, I.; Wikberg, J. E. *N*-Hydroxyguanidine compound 1-(3,4-dimethoxy-2-chlorobenzylideneamino)-3-hydroxyguanidine inhibits the xanthine oxidase mediated generation of superoxide radical. *Arch. Biochem. Biophys.* **2000**, *377*, 101−108.
(27) Veveris, M.; Dambrova, M.; Cirule, H.; Meirena, D.; Kalvinsh, I.; Wikberg, J. E. Cardioprotective effects of *N*-hydroxyguanidine PR5 in myocardial ischaemia and reperfusion in rats. *Br. J. Pharmacol.* **1999**, *128*, 1089−1097.
(28) Doubell, P. C. J.; Oliver, D. W.; van Rooyen, P. H. 1-(Benzylideneamino)-3-hydroxyguanidinium tosylate. *Acta Crystallogr.* **1991**, *C47*, 353−355.
(29) Pastor, M.; Cruciani, G.; McLay, I.; Pickett, S.; Clementi, S. GRid-INdependent descriptors (GRIND): a novel class of alignment-independent three-dimensional molecular descriptors. *J. Med. Chem.* **2000**, *43*, 3233−3243.
(30) Dambrova, M.; Veveris, M.; Cirule, H.; Pugovichs, O.; Post, C.; Lundstedt, T.; Kalvinsh, I.; Skottner, A.; Wikberg, J. E. The novel guanidine ME10092 protects the heart during ischemia−reperfusion. *Eur. J. Pharmacol.* **2002**, *445*, 105−113.
(31) Ledoux, F.; Welsch, M.; Steimer, C.; Schwartz, J. A clinical trial of guanoxabenz: a hypotensive agent with central and hypertensive action. *Therapie* **1981**, *36*, 187−191.
(32) Tai, A. W.; Lien, E. J.; Lai, M. M. C.; Khwaja, T. A. Novel *N*-hydroxyguanidine derivatives as anticancer and antiviral agents. *J. Med. Chem.* **1984**, *27*, 236−238.
(33) Tang, A.; Lien, E. J.; Lai, M. M. C. Optimization of the Schiff bases of *N*-hydroxy-*N*′-aminoguanidine as anticancer and antiviral agents. *J. Med. Chem.* **1985**, *28*, 1103−1106.
(34) Pignatello, R.; Panico, A.; Mazzone, R.; Pinizzotto, M. R.; Carozzo, A.; Furneri, P. M. Schiff bases of *N*-hydroxy-*N*′-aminoguanidines as antiviral, antibacterial and anticancer agents. *Eur. J. Med. Chem.* **1994**, *29*, 781−785.
(35) Doubell, P. C. J.; Oliver, D. W. Synthesis and anti-HIV-1 activity of N-hydroxy-N1-aminoguanidines. *Arzneim.-Forsch.* **1992**, *42*, 65−69.
(36) Wang, P.-H.; Keck, G. J.; Lien, E. J.; Lai, M. M. C. Design, synthesis, testing, and quantitative structure−activity relationship analysis of substituted salicylaldehyde Schiff bases of 1-amino-3-hydroxyguanidine tosylate as new antiviral agents against coronavirus. *J. Med. Chem.* **1990**, *33*, 608−614.
(37) Lien, E. J. *Prog. Drug Res.* **1993**, *40*, 163.
(38) *SYBYL*, version 6.5; Tripos Inc., 1699 South Hanley Road, St. Louis, Missouri, 63144.
(39) Allen, F. H.; Kennard, O. 3D Search and Research Using the Cambridge Structural Database. *Chem. Des. Autom. News* **1993**, *8* (1), 31−37.
(40) Stewart, J. J. P. Optimization of Parameters for Semiempirical Methods II. Methods. *J. Comput. Chem.* **1989**, *10*, 209−220.
(41) Stewart, J. J. P. Optimization of Parameters for Semiempirical Methods II. Applications. *J. Comput. Chem.* **1989**, *10*, 221−264.
(42) Stewart, J. J. P. MOPAC, A Semi-Emiprical Molecular Orbital Program. *Quantum Chem. Program Exch.* **1983**, 455.
(43) *ALMOND*, version 2.0; MIA S.r.l., Viale dei Castagni 16, I-06143 Perugia, Italy.
(44) Goodford, P. J. A computational procedure for determining energetically favourable binding sites on biologically important macromolecules. *J. Med. Chem.* **1985**, *28*, 849−857.
(45) Geladi, P.; Kowalski, B. R. Partial least-squares regression: A tutorial. *Anal. Chim. Acta* **1986**, *185*, 1−17.
(46) Baroni, M.; Constantino, G.; Cruciani, G.; Riganelli, D.; Valigi, R.; Clementi, S. Generating optimal linear PLS estimations (GOLPE): an advanced chemometric tool for handling 3D-QSAR problems. *Quant. Struct.−Act. Relat.* **1993**, *12*, 9−20.
(47) Wakeling, I. N.; Morris, J. J. A test of significance for partial least squares regression. *J. Chemom.* **1993**, *7*, 291−304.

JM031127C